Posttranslational mechanisms associated with reduced NHE3 activity in adult vs. young prehypertensive SHR

Renato O. Crajoinas,[1] Lucília M. A. Lessa,[2] Luciene R. Carraro-Lacroix,[3] Ana Paula C. Davel,[2] Bruna P. M. Pacheco,[1] Luciana V. Rossoni,[2] Gerhard Malnic,[2] and Adriana C. C. Girardi[1]

[1]Heart Institute (InCor), Medical School, [2]Department of Physiology and Biophysics, Institute of Biomedical Sciences, University of São Paulo; and [3]Department of Physiology, Federal University of São Paulo, São Paulo, Brazil

Crajoinas RO, Lessa LMA, Carraro-Lacroix LR, Davel APC, Pacheco BPM, Rossoni LV, Malnic G, Girardi ACC. Posttranslational mechanisms associated with reduced NHE3 activity in adult vs. young prehypertensive SHR. *Am J Physiol Renal Physiol* 299: F872–F881, 2010. First published July 14, 2010; doi:10.1152/ajprenal.00654.2009.—Abnormalities in renal proximal tubular (PT) sodium transport play an important role in the pathophysiology of essential hypertension. The Na^+/H^+ exchanger isoform 3 (NHE3) represents the major route for sodium entry across the apical membrane of renal PT cells. We therefore aimed to assess in vivo NHE3 transport activity and to define the molecular mechanisms underlying NHE3 regulation before and after development of hypertension in the spontaneously hypertensive rat (SHR). NHE3 function was measured as the rate of bicarbonate reabsorption by means of in vivo stationary microperfusion in PT from young prehypertensive SHR (Y-SHR; 5-wk-old), adult SHR (A-SHR; 14-wk-old), and age-matched Wistar Kyoto (WKY) rats. We found that NHE3-mediated PT bicarbonate reabsorption was reduced with age in the SHR (1.08 ± 0.10 vs. 0.41 ± 0.04 nmol/cm²×s), while it was increased in the transition from youth to adulthood in the WKY rat (0.59 ± 0.05 vs. 1.26 ± 0.11 nmol/cm²×s). Higher NHE3 activity in the Y-SHR compared with A-SHR was associated with a predominant microvilli confinement and a lower ratio of phosphorylated NHE3 at serine-552 to total NHE3 (P-NHE3/total). After development of hypertension, P-NHE3/total increased and NHE3 was retracted out of the microvillar microdomain along with the regulator dipeptidyl peptidase IV (DPPIV). Collectively, our data suggest that the PT is playing a role in adapting to the hypertension in the SHR. The molecular mechanisms of this adaptation possibly include an increase of P-NHE3/total and a redistribution of the NHE3-DPPIV complex from the body to the base of the PT microvilli, both predicted to decrease sodium reabsorption.

sodium transport; proximal tubule; blood pressure; phosphorylation; dipeptidyl peptidase IV

MAINTENANCE OF EXTRACELLULAR volume homeostasis depends upon the kidneys to precisely balance sodium excretion with dietary sodium intake. To accomplish this task, the activities of a number of sodium transport proteins along the nephron are tightly regulated. The proximal tubule (PT) accounts for reabsorption of ~65% of the filtered water and of most solutes. The Na^+/H^+ exchanger isoform 3 (NHE3) represents the major route for sodium entry and H^+ secretion in this nephron segment (5, 6, 30, 37, 40–42). NHE3 also has a major role in mediating NaCl reabsorption in the PT through its combined activity with a Cl^-/base exchanger (2, 43) and by creating an increase in luminal chloride concentration that favors the diffusion of the anion from the tubular lumen to the blood. NHE3-mediated Na^+/H^+ exchange is therefore the predominant PT mechanism for $NaHCO_3^-$ and NaCl reabsorption.

Micropuncture analysis on NHE3 knockout mice revealed a remarkable reduction of PT fluid (~60%) and bicarbonate (~50%) reabsorption (30, 40–42). Consequently, mice lacking NHE3 exhibit reduced blood pressure, mild acidosis, elevated serum aldosterone, and elevated mRNA encoding renal renin. Despite a chronic volume-depleted state, NHE3 knockouts fed on a regular sodium diet are viable mostly due to reduced glomerular filtration rate (GFR) and increased sodium and bicarbonate reabsorption in the distal nephron (27, 37). Nevertheless, when these mice are submitted to dietary sodium restriction, the adaptive responses are not sufficient to fully compensate for the large defect on PT reabsorption, and they display significant urinary sodium wasting and sharply reduced blood pressure and may undergo hypovolemic shock (27).

Given the important role of NHE3 in mediating sodium and fluid reabsorption, this transporter is subject to acute and chronic regulation in response to a variety of conditions affecting salt balance, including volume contraction (9), high salt intake (33, 45), and hypertension (16, 21, 25, 46). Using an experimental animal model of chronic volume contraction, Fisher et al. (9) observed that NHE3 expression is significantly upregulated in the renal cortex at both protein and mRNA levels. As part of the kidney's natriuretic response to restore volume homeostasis, NHE3 activity is downregulated in rats fed a high-sodium diet (33). Reduced NHE3 activity in response to high-sodium intake is associated with increased levels of NHE3 phosphorylated at serine-552 and redistribution of the transporter out of the brush-border microvilli (MMV), a transport-relevant domain of apical membrane, together with its associated protein dipeptidyl peptidase IV (DPPIV) (45).

Conflicting data have been reported with regard to NHE3 modulation in genetic models of essential hypertension. Studies using ex vivo (25) and in vitro (21) approaches have shown that NHE3 activity is upregulated at all stages of hypertension in spontaneously hypertensive rats (SHR). Conversely, studies by the McDonough and Yip laboratories (31, 44, 46) have consistently reported that NHE3 is redistributed from the body to the base of the MMV in this rat lineage during the hypertensive stage. This shift is accompanied by increases of lithium clearance, a marker for volume flow out of the PT (31), suggesting that NHE3 redistribution is associated with decreased PT sodium reabsorption. If so, rather than contributing to development and maintenance of hypertension, NHE3 plays a protective role counterbalancing blood pressure rising in the A-SHR.

Address for reprint requests and other correspondence: A. C. C. Girardi, Institute of Heart, Laboratory of Genetics and Molecular Cardiology, Univ. of São Paulo Medical School, Avenida Dr. Enéas de Carvalho Aguiar, 44, 10° andar, Bloco II, 05403-900, São Paulo, SP, Brazil (e-mail: adriana.girardi @incor.usp.br).

In the present report, in vivo stationary microperfusion was employed to assess NHE3 transport function in the native PT of young prehypertensive and adult hypertensive SHR. Molecular mechanisms known to be important in regulation of NHE3, including direct protein phosphorylation and subcellular redistribution with the interacting protein DPPIV, were also investigated before and after development of hypertension in the SHR strain.

MATERIALS AND METHODS

Reagents and antibodies. Reagents were obtained from Sigma (St. Louis, MO) unless otherwise specified. S3226 was a gift from Sanofi-Aventis (Frankfurt, Germany). A monoclonal antibody (mAb) to rat DPPIV, clone 5E8, a mouse mAb anti-PS552, clone 14D5 (23), as well as goat-polyclonal anti-villin were purchased from Santa Cruz Biotechnology (Santa Cruz, CA). mAb raised to the renal brush-border NHE3 (6) was purchased from Millipore (Billerica, MA) and mAb to actin (JLA20) was purchased from Merck (Darmstadt, Germany). A rabbit polyclonal anti-megalin antibody was kindly provided by Dr. Daniel Biemesderfer at Yale University, New Haven, CT. Horseradish peroxidase-conjugated goat anti-mouse, goat anti-rabbit, and rabbit anti-goat secondary antibodies were purchased from Invitrogen (San Diego, CA).

Animal protocols. Animal procedures and protocols were followed in accordance with the ethical principles in animal research of the Brazilian College of Animal Experimentation and were approved by the institutional animal care and use committee. Experiments were performed using young (5-wk-old) and adult (14-wk-old) male SHRs and age-matched normotensive control Wistar-Kyoto (WKY) rats. Rats were housed under standardized conditions (constant temperature of 22°C, 12:12-h light-dark cycle, and relative humidity of 60%) at the University of São Paulo Medical School animal facility. Blood pressure in conscious restrained rats was measured noninvasively by tail cuff plethysmography (BP-2000 Blood Pressure Analysis System; Visitech Systems, Apex, NC). Prior to these measurements, rats were trained in the blood pressure device to become adapted to the experimental procedures and to renal function assessment, rats were placed in metabolic cages during three consecutive days. Urine samples collected during each 24-h period were used to determine urinary flow, GFR, urinary sodium excretion, and endogenous lithium clearance. Arterial blood samples were collected from carotid arteries at the time of death for measurements of sodium, lithium, and creatinine concentration. Sodium was measured on a 9180 Electrolyte Analyzer (Roche Diagnostics, Mannheim, Germany). Flame photometry (model B262; Micronal, São Paulo, Brazil) was performed to obtain lithium concentrations. Creatinine was measured on a Synchron CX7 Analyzer (Beckman Coulter, Fullerton, CA). Creatinine clearance was used to estimate GFR. Endogenous lithium clearance was calculated as $V \times U_{Li}/P_{Li}$ where V is urine output, U_{Li} is urinary lithium concentration, and P_{Li} is plasma lithium concentration.

In vivo stationary microperfusion. Rats were anesthetized by intramuscular administration of tiletamine-zolazepam (30 mg/kg). The left jugular vein was cannulated for infusion of mannitol-saline at a rate of 0.1 ml/min. The kidney was exposed by a lumbar approach and prepared for in vivo micropuncture. PTs were perfused by means of double-barreled micropipettes: one barrel was filled with Sudan Black colored castor oil, and the other, with an FDC green-colored solution of 100 mm NaCl and 25 mm NaHCO$_3^-$ (perfusion solution). To minimize fluid reabsorption, this solution had been rendered isotonic through the addition of raffinose. The rate of tubular acidification was measured by injecting a droplet of the perfusion solution between the oil columns and following the luminal pH changes toward the steady-state level (stationary perfusion). Luminal pH was measured by means of double-barreled microelectrodes, one barrel being filled with H$^+$ ionophore (cocktail B; Fluka, Buchs, Switzerland) and the other with

reference solution colored by FDC green. The voltage between the microelectrode barrels, representing luminal H$^+$ activity, was continuously recorded with a microcomputer equipped with an analog-to-digital conversion board (Lynx, São Paulo, Brazil) for data acquisition and processing. Bicarbonate concentration was calculated from pH and from measured arterial Pco$_2$. The rate of tubular acidification was calculated as the half-time of the reduction of the injected HCO$_3^-$ concentration to its stationary level ($t_{1/2}$). The net bicarbonate reabsorption ($J_{HCO_3^-}$) was then calculated using the following equation (8)

$$J\text{HCO}_3^- = \frac{\ln 2}{t_{1/2}}[(\text{HCO}_3^-)_0 - (\text{HCO}_3^-)_s] \times \frac{r}{2}$$

where $t_{1/2}$ is the acidification half-time; $(\text{HCO}_3^-)_0$ and $(\text{HCO}_3^-)_s$ are the injected concentration of bicarbonate and steady-state bicarbonate concentration respectively; and r is the tubular radius.

Real-time RT-PCR. Total RNA was isolated from renal cortices as previously described (36). First-strand cDNA synthesis was performed with Super-Script III Reverse Transcriptase following the manufacturer's guidelines. Fifteen nanogram cDNAs were used for real-time RT-PCR reaction (SYBR Green PCR Master Mix-PE; Applied Biosystems) in an ABI Prism 7700 Sequence Detection System (Applied Biosystems). All samples were assayed in triplicate. The control gene 28S ribosomal RNA was used to normalize the results. The comparative threshold cycle method was used for data analyses. Oligonucleotide primers used were as follows: NHE3, 5′-ACTGCTTA-ATGACGCGGTGACTGT-3′ (forward) and 5′-AAAGACGAAGCCAGGCTCGATGAT-3′ (reverse); and 28S, 5′-TCATCAGACCCCAGAAAAGG-3′ (forward) and 5′-GATTCGGCAGGTGAGTTG-3′ (reverse).

Isolation of renal cortical microsomes. Rats were euthanized by intraperitoneal injection of pentobarbital sodium. Kidney cortices were isolated at 4°C and homogenized in PBS containing 1 tablet/50 ml of complete protease inhibitor cocktail tablets (Roche, Mannheim, Germany) and phosphatase inhibitors (50 mM NaF and 15 mM sodium pyrophosphate) at pH 7.4. The homogenate was centrifuged at 2,000 g for 15 min at 4°C. The supernatant was removed and subjected to a further 1 h of centrifugation at 100,000 g at 4°C to pellet the microsomal fraction. The supernatant was discarded, and the microsomes were resuspended in fresh PBS containing protease and phosphatase inhibitors.

Microvillar membrane vesicle preparation. Rat kidney cortices were isolated at 4°C and homogenized in a K-HEPES buffer (200 mM mannitol, 80 mM HEPES, 41 mM KOH, pH 7.5) containing protease and phosphatase inhibitors (as above). Microvillus membrane vesicles were prepared using a method based on Mg^{2+} precipitation and differential centrifugation as described previously (1).

Preparation of renal membrane fractions. Postmitochondrial renal cortical microsomes were prepared and separated on 15–30% Opti-Prep (Nycomed Pharma, Oslo, Norway) gradients, essentially as described previously (4). One-milliliter fractions were manually collected from the top and assayed by immunoblotting for the presence of villin, megalin, NHE3, and DPPIV. Figure 1 illustrates the density separation of cortical microsomes from an 14-wk-old WKY (A-WKY) rat obtained by isopycnic centrifugation. *Fraction 1*, which was enriched in the microvillar membrane marker villin (low-density gradient fraction), was pelleted by centrifugation and resuspendend in K-HEPES buffer. High-density fractions, which were enriched in megalin were pooled from *fractions 5–6* in the gradient, pelleted, and then resuspended in K-HEPES buffer. The same procedure was repeated to prepare membrane fractions from Y- and A-SHR and of Y-WKY rats (data not shown).

SDS-PAGE and immunoblotting. Proteins were solubilized in SDS-PAGE sample buffer and subjected to SDS-PAGE using 7.5% polyacrylamide gels. Proteins were subsequently transferred to polyvinylidene fluoride membranes (Immobilon-P; Millipore). Nonspecific binding was blocked by incubating the polyvinylidene fluoride membrane at room temperature for 1 h in Blotto (5% nonfat dry milk and
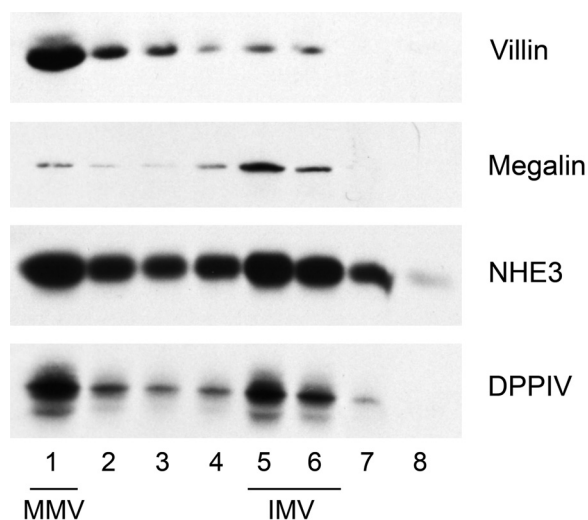
Fig. 1. Density separation of renal cortical microsomes from adult Wistar-Kyoto (A-WKY) rats. Renal cortical microsomes were separated by isopycnic centrifugation using 15–30% OptiPrep density gradients. Fractions (1 ml) were collected across the gradient, and 25 μl of each was prepared for SDS-PAGE and immunoblotting. *Fraction 1* represents the top (lightest fraction) and *fraction 8* represents the bottom (densest fraction) of the gradient. The same blot was probed successively with antibodies for megalin, villin, Na$^+$/H$^+$ exchanger isoform 3 (NHE3), and dipeptidyl peptidase IV (DPPIV). *Fraction 1* [microvillus (MMV) membranes], which was enriched in the MMV membrane marker villin, was pelleted by centrifugation. Dense vesicles [intermicrovilli vesicles (IMV)], which are enriched in megalin, were pooled from *fractions 5–6* in the gradient.

0.1% Tween 20 in PBS, pH 7.4) followed by overnight incubation with 1:1,000 anti-PS552 (23), 1:1,000 anti-NHE3 (6), 1:1,000 anti-DPPIV, 1:50,000 anti-megalin, or 1:50,000 anti-actin at 4°C in Blotto. The membranes were then washed five times with Blotto and incubated for 1 h with horseradish peroxidase-conjugated immunoglobulin secondary antibody (1:2,000). Membranes were again washed five times with Blotto and then rinsed in PBS. Bound antibody was detected with enhanced chemiluminescence (GE Healthcare) according to the manufacturer's protocols. The visualized bands were digitized using the ImageScanner III (GE HealthCare) and quantified using Image software (Scion, Frederick, MD). The amount of sample to optimally detect phosphorylated NHE3, total NHE3, and actin in the linear range was chosen based on the experiments shown in supplementary Fig. S1 (supplemental data for this article are available online at the *American Journal of Physiology–Renal Physiology* website.).

Statistics. All results are reported as means ± SE with *n* indicating the number of observations. Comparisons between two groups were performed using unpaired *t*-tests. If more than two groups were compared, statistical significance was determined by ANOVA followed by Tukey's post hoc test. A *P* value < 0.05 was considered significant. The program "Graph Pad Prism 5" (Graph Pad Software, San Diego, CA) was used to calculate significance.

RESULTS

Blood pressure and renal function. Blood pressure in SHR and WKY rats was measured by tail cuff plethysmography. As depicted in Table 1, systolic blood pressure was slightly but significantly higher in 5-wk-old SHR (Y-SHR) than in age-matched Y-WKY (113 ± 4 vs. 91 ± 2 mmHg, *P* < 0.05), whereas adult SHR (A-SHR) had markedly higher systolic blood pressure than a A-WKY (189 ± 5 vs. 106 ± 4 mmHg, *P* < 0.001). Although systolic blood pressure was elevated in Y-SHR compared with the normotensive control, these rats had not yet developed hypertension. Fourteen-week-old A-SHRs, on the other hand, were already hypertensive.

Urine output, GFR, urinary sodium excretion, and lithium clearance were significantly lower in Y-SHR compared with Y-WKY (Table 1). The mean values of urine output, sodium excretion, and GFR were lower in A-SHR relative to A-WKY, but none of these parameters reached statistical significance. Conversely, lithium clearance was significantly higher in the A-SHR (*P* < 0.001 vs. A-WKY) (Table 1).

PT NHE3-mediated bicarbonate reabsorption. The in vivo NHE3 transport activity was measured as the rate of bicarbonate reabsorption in the native PT by means of stationary microperfusion. Experiments were performed either in the presence or absence of 2 μM S3226, a selective NHE3 inhibitor (38). Figure 2*A* attests that the rate of bicarbonate flux ($J_{HCO_3^-}$) in luminal-perfused PTs of Y-SHR was significantly higher than in Y-WKY (1.9 ± 0.19 vs. 1.36 ± 0.13 nmol/cm^2×s, *P* < 0.05). Elevated NHE3 transport activity did not persist during SHR adulthood. As seen in Fig. 2*A*, PT bicarbonate reabsorption was significantly lower in A-SHR compared with A-WKY (1.21 ± 0.09 vs. 2.04 ± 0.19 nmol/cm^2×s, *P* < 0.001). The S3226-insensitive bicarbonate reabsorption component was equivalent between these two rat strains. The difference in $J_{HCO_3^-}$ between SHR and WKY was even more pronounced when only the NHE3-mediated-bicarbonate reabsorption was taken into account (the S3226-sensitive component of PT bicarbonate reabsorption, i.e., total reabsorption minus reabsorption in the presence of S3226) (Fig. 2*B*). Results shown in Fig. 2*B* demonstrate that in vivo NHE3 transport

Table 1. *Body weight, blood pressure, and renal function of spontaneously hypertensive rats (SHRs) and Wistar-Kyoto (WKY) rats at 5 wk (Y) and 14 wk of age (A)*

	Y-WKY	Y-SHR	A-WKY	A-SHR
Body Weight, g	132 ± 5 (16)	98 ± 3* (18)	301 ± 8 (16)	272 ± 5* (16)
SBP, mmHg	91 ± 2 (12)	113 ± 4* (18)	106 ± 4 (15)	189 ± 5* (16)
Urine output, μl·min^{-1}·kg^{-1}	52 ± 4 (12)	34 ± 2* (18)	37 ± 2 (15)	31 ± 2 (16)
GFR, ml·min^{-1}·kg^{-1}	8.8 ± 0.4 (12)	7.9 ± 0.3* (18)	6.3 ± 0.4 (16)	5.9 ± 0.4 (16)
Urinary Na$^+$, meq·min^{-1}·kg^{-1}	8.6 ± 0.3 (12)	5.7 ± 0.2* (18)	5.6 ± 0.4 (16)	5.2 ± 0.3 (16)
Li$^+$ clearance, μl·min^{-1}·kg^{-1}	161 ± 14 (12)	116 ± 4* (18)	69 ± 4 (15)	103 ± 10* (16)

Values are means ± SE. Number in parentheses is number of animals per group. Systolic blood pressure (SBP) was measured noninvasively by tail cuff plethysmography. Rats were placed in metabolic cages for collection of 24-h urine samples. Urine output was measured gravimetrically. Creatinine clearance was used to estimate glomerular filtration rate (GFR). Renal functional data were corrected by body weight and expressed as grams per kilogram body wt. *P* < 0.01 vs. age matched WKY.
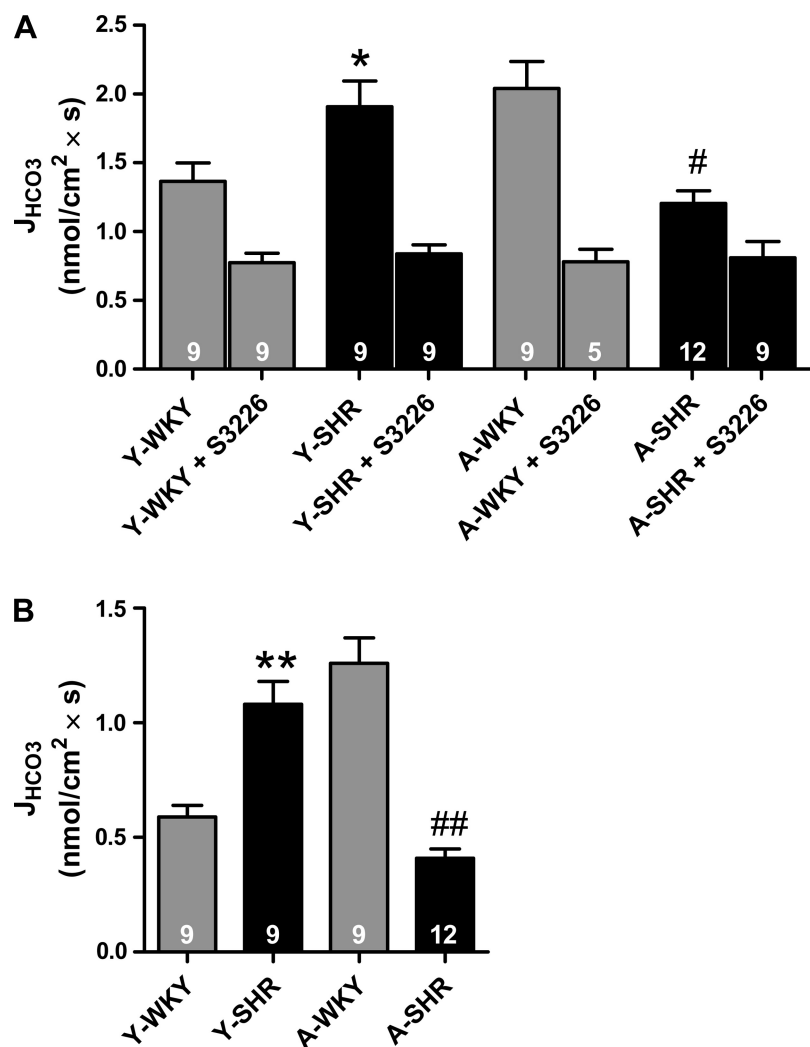
A

B

Fig. 2. Bicarbonate reabsorption ($J_{HCO_3^-}$) in renal proximal tubule (PT) from membranes from 5-wk-old SHR (Y-SHR), 14-wk-old SHR (A-SHR), and age-matched WKY rats. $J_{HCO_3^-}$ was evaluated by means of stationary microperfusion and continuous measurement of luminal pH in the absence or presence of 2 μM S3226. Numbers of perfused tubules are indicated in the bars. Data are means ± SE. *$P < 0.05$; **$P < 0.001$ vs. Y-WKY; #$P < 0.05$; ##$P < 0.001$ vs. A-WKY. Renal PT $J_{HCO_3^-}$ (A) and S3226-sensitive component of PT $J_{HCO_3^-}$ (B) are shown.

activity was 83 ± 7% higher in Y-SHR than in Y-WKY ($P < 0.001$) and 67 ± 5% lower in A-SHR compared with A-WKY ($P < 0.001$). In Table 2, the data presented above is displayed and statistically analyzed with regard to age-dependent changes on NHE3 function. Interestingly, NHE3 activity was reduced in the transition from Y-SHR to A-SHR (62 ± 6%), while it was increased in the transition between Y-WKY and A-WKY (113 ± 10%) (Fig. 2B, Table 2).

*Renal cortical NHE3-mRNA expression.* The relative amount of NHE3-mRNA in renal cortex from SHR and WKY rats was determined by real-time RT-PCR using specific primers corresponding to the rat NHE3 COOH-terminal region. The expression of NHE3 transcript was normalized by 28S-RNA. As depicted in Table 2, the expression levels of NHE3-mRNA in renal cortex did not vary significantly between SHR and WKY at both 5 and 14 wk of age. Table 2 also shows that NHE3-mRNA expression was significantly higher in both A-SHR and A-WKY rats relative to their young counterparts. This pattern is also consistently observed at the protein level (Table 2, Fig. 3, *A* and *B*), as previously reported by Magyar et al. (31).

Table 2. *Age-dependent changes on proximal tubular Na$^+$/H$^+$ exchanger isoform 3 (NHE3) transport activity and NHE3-mRNA, protein expression and endogenous phosphorylation levels in renal cortex of SHR and WKY rats*

	Y-WKY	A-WKY	Y-SHR	A-SHR
Transport activity, nmol/cm^2×s	0.59 ± 0.05 (9)	1.26 ± 0.11* (9)	1.08 ± 0.10 (9)	0.41 ± 0.04* (12)
mRNA levels, AU	0.27 ± 0.03 (3)	0.57 ± 0.05* (3)	0.23 ± 0.04 (3)	0.53 ± 0.06* (3)
Protein abundace, AU	0.76 ± 0.09 (5)	1.11 ± 0.07* (5)	0.78 ± 0.09 (5)	1.14 ± 0.09* (5)
P-NHE3/total, AU	0.57 ± 0.01 (5)	0.32 ± 0.02* (5)	0.35 ± 0.01 (5)	0.60 ± 0.02* (5)

Values are means ± SE. Number in parentheses is number of perfused tubules or animals per group. Proximal tubular (PT) NHE3 transport activity was measured by stationary in situ microperfusion and is expressed as the mean values of the S3226-sensitive component of PT bicarbonate reabsorption. NHE3-mRNA was measured by real-time PCR and 28S-RNA was used as internal control. Total and phosphorylated NHE3 (P-NHE3) were assessed by immunoblotting in renal cortical microsomes. The mean values of relative NHE3 expression normalized to actin and of the phosphorylated NHE3 to total NHE3 ratio (P-NHE3/total) are expressed in arbitrary units (AU). *$P < 0.001$ vs. young counterpart assessed by unpaired *t*-test.

Fig. 3. Expression of total and phosphorylated Na$^+$/H$^+$ exchanger isoform 3 (P-NE3) at serine-552 in renal cortical microsomes from Y-SHR, A-SHR, and age-matched WKY rats. Equivalent samples (15 μg for NHE3; 5 μg for PS552-NHE3, and 2.5 μg for actin) of renal cortical microsomes isolated from A- and Y-SHR and WKY rats were subjected to SDS-PAGE, transferred to a polyvinylidene fluoride (PVDF) membrane and analyzed by immunoblotting. *A*: representative immunoblot of NHE3 phosphorylation and expression in renal cortical microsomes. Membranes were incubated with monoclonal antibodies against P-NHE3 at serine-552 (1:1,000), total NHE3 (1:1,000), and anti-actin (1:50,000). Graphical representation of the relative expression levels of total NHE3 normalized to actin (*B*) and of the ratio of P-NHE3 at serine-552 to total NHE3 (P-NHE3/total) (*C*) in renal cortical microsomes. Values are means ± SE; *n* = 5/group, *P < 0.001 vs. Y-WKY; #P < 0.001 vs. A-WKY.
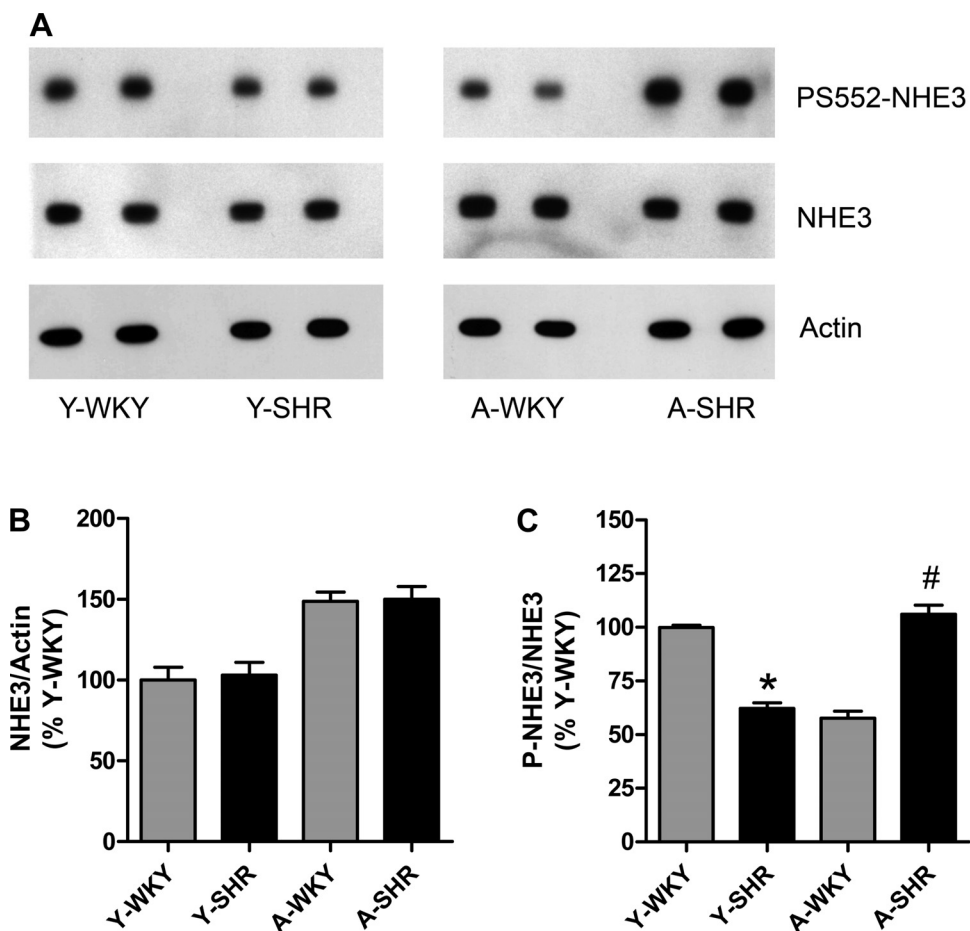
Expression of total and phosphorylated NHE3 at serine-552 in renal cortical microsomes. Examination of the phosphorylation status of NHE3 was performed by immunoblotting by using a phosphospecific monoclonal antibody that recognizes NHE3 only when it is phosphorylated at serine-552 (23). As seen in Fig. 3, *A* and *C*, the relative ratio of phosphorylated NHE3 at serine-552 to total NHE3 (P-NHE3/total) was lower in renal cortical microsomes from Y-SHR compared with Y-WKY (61 ± 3%, P < 0.001). In contrast, A-SHR displayed higher P-NHE3/total in renal cortex than A-WKY (87 ± 3%, P < 0.001). The results shown in Figs. 2–3 and in Table 2 demonstrate that changes on the P-NHE3/total ratio in renal cortical microsomes from SHR and WKY rats inversely correlated with changes on NHE3 function. When considering this ratio in terms of age dependence, it is noticeable that the P-NHE3/total ratio increases with age in SHR (71 ± 2%, P < 0.001), whereas it decreases from youth to adulthood in the WKY (56 ± 2%, P < 0.001) (Table 2, Fig. 3C).

Expression of total and P-NHE3 in PT MMV membranes vesicles. The NHE3 phosphorylation status and protein content were also evaluated within the PT brush-border MMV prepared from SHR or WKY rats. Figure 4 shows that total NHE3 expression in Y-SHR MMV membranes was higher (56 ± 7%, P < 0.001) and that the relative ratio of P-NHE3/total was significantly lower than in Y-WKY (64 ± 3%, P < 0.001) group. After development of hypertension, A-SHR exhibited lower MMV NHE3 expression (69 ± 6%, P < 0.001) (Fig. 4,

A and *B*) and a higher P-NHE3/total ratio (71 ± 5%, P < 0.001) than A-WKY (Fig. 4, *A* and *C*).

Subcellular distribution of NHE3 and DPPIV. The distribution of NHE3 and DPPIV within the brush-border subcompartments was evaluated in SHR and WKY by means of subcellular fractionation and immunoblotting. The immunoblotting experiments were performed using equal amounts of protein from either MMV or intermicrovilli (IMV) separated from SHR and WKY rats as described in MATERIALS AND METHODS. Illustrated in Fig. 5, *A–D*, villin is predominantly expressed in MMV, while megalin is more highly expressed in the IMV than in the MMV domain. The distribution of these markers did not alter with respect to either age or rat strain. As shown in Fig. 5, *E* and *F*, NHE3 was practically equally distributed between the MMV and IMV microdomains in both Y- and A-WKY. As previously determined by microscopy (46) and density gradient fractionation (31), this pattern of distribution was altered in the SHR. Consistent with the immunoblotting experiments using microvillus membrane vesicles isolated by divalent cation precipitation (Fig. 4), we found that NHE3 was predominantly confined to the MMV microdomain of the PT brush-border in Y-SHR (Fig. 5E). In contrast, A-SHR exhibited higher NHE3 expression in the IMV-enriched fraction (Fig. 5F). As observed in Fig. 5, *G* and *H*, DPPIV is much more abundant in MMV than in IMV in both SHR and WKY. However, the distribution of this peptidase discretely changes between these brush-border subcompartments in the SHR
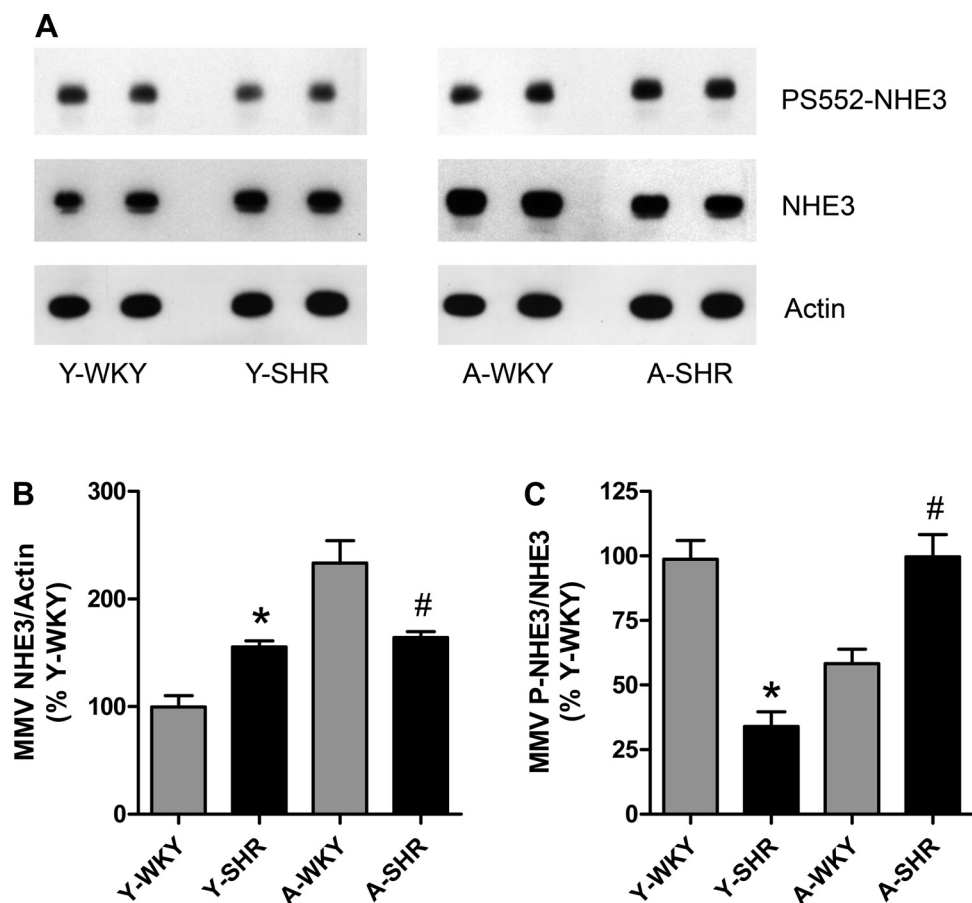
Fig. 4. Expression of total and P-NHE3 at serine-552 in brush-border MMV membranes from Y-SHR, A-SHR, and age-matched WKY rats. Equivalent samples (15 μg for NHE3; 5 μg for PS552-NHE3, and 2.5 μg for actin) of MMV prepared by divalent cation aggregation from WKY and SHR were subjected to SDS-PAGE, transferred to a PVDF membrane, and analyzed by immunoblotting. *A*: representative immunoblot of NHE3 phosphorylation and expression in kidney MMV. The membranes were incubated with monoclonal antibodies against P-NHE3 at serine-552 (1:1,000), total NHE3 (1:1,000), and anti-actin (1:50,000). Graphical representation of the relative expression levels of total NHE3 normalized to actin (*B*) and of the ratio of P-NHE3/total (*C*) in microvillar membranes. Values are means ± SE; $n = 5$/group, $*P < 0.001$ vs. Y-WKY; $\#P < 0.001$ vs. A-WKY.

strain. In the Y-SHR, 81% of DPPIV is confined to the MMV, while 19% resides in the IMV-enriched fraction. Microvillar DPPIV expression was slightly but significantly higher in Y-SHR than in Y-WKY (16 ± 1%, $P < 0.01$) and lower in A-SHR vs. A-WKY (18 ± 2%, $P < 0.01$). With regard to age-related changes in DPPIV distribution, we found that the percentage of the peptidase that resides in the MMV microdomain decreased from 81 to 65%, and the one that is confined to the IMV increased from 19 to 35% in the transition from youth to adulthood in the SHR. The distribution of DPPIV did not differ significantly with age in the WKY rats.

DISCUSSION

Results presented here indicate that the NHE3 transport function is higher in the PT of SHR prior to the development of hypertension and lower thereafter compared with the age-matched normotensive WKY rats. Remarkably, NHE3 activity is reduced with age in the SHR, while it is increased in the transition between Y- and A-WKY. Higher NHE3 activity in the prehypertensive Y-SHR (compared to either Y-WKY or A-SHR) is accompanied by enhanced NHE3 expression in the brush-border MMV, where the transporter physically associates with the regulator DPPIV (10) and lower phosphorylation levels of serine-552. In the A-SHR, all of these regulatory mechanisms seem to work in an opposite fashion to reduce PT sodium reabsorption. Our data are consistent with the notion that enhanced PT NHE3 activity contributes to the onset of hypertension in the Y-SHR (16, 21, 25, 39). Nevertheless, once

hypertension is established, reduced NHE3 activity represents an integral part of the pressure-natriuresis response to counteract blood pressure rising (31, 44, 46).

Sodium retention and volume expansion play an important role in the pathogenesis of essential hypertension (32). Our data show that renal function is substantially altered in the prehypertensive Y-SHR. These animals exhibited lower GFR, which led to less sodium to be filtered and excreted compared with age-matched WKY rats. Besides, lithium clearance was reduced, suggesting that PT sodium reabsorption is increased. By means of stationary in situ microperfusion, we found that NHE3-mediated bicarbonate reabsorption was ~80% higher in 5-wk-old SHR compared with age-matched WKY. These data confirm previous reports describing elevation of NHE3 activity before onset of hypertension in genetic models of essential hypertension (16, 21, 25, 39).

Once hypertension is established, the differences between A-SHR and A-WKY rats with respect to urine output, urinary sodium excretion, and GFR are much more attenuated and do not reach statistical significance. However, lithium clearance is increased, suggesting that PT sodium reabsorption is lower. Accordingly, NHE3-mediated bicarbonate reabsorption in renal PT was ~70% diminished in the hypertensive A-SHR compared with age-matched WKY. Our findings are in contrast to those of LaPointe et al. (25) and Kobayashi et al. (21) who demonstrated that NHE3 activity persists, stimulated after development of hypertension in SHR. Such discrepancy is likely attributed to the fact that our functional studies were
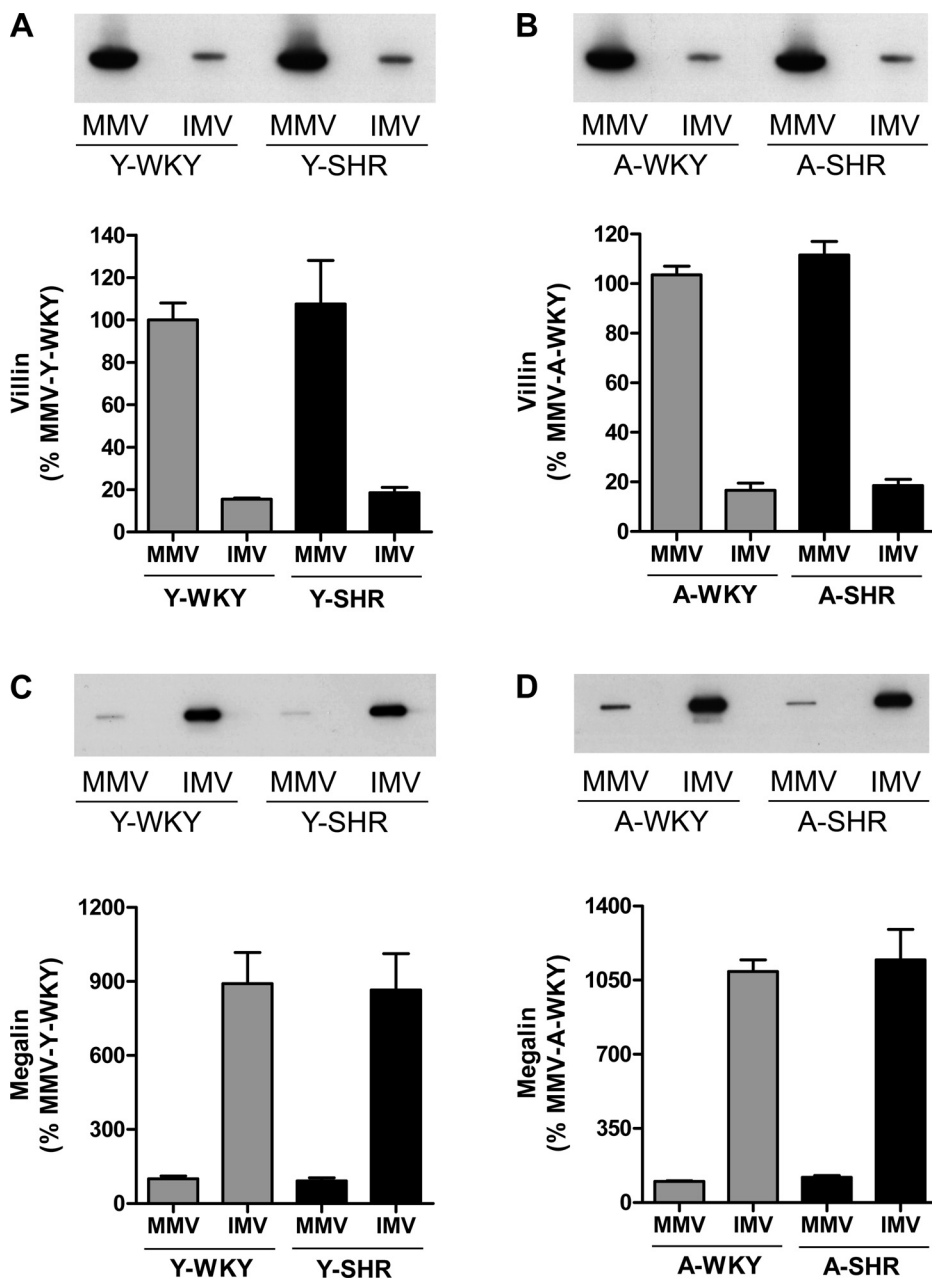
Fig. 5. Distribution of NHE3 and DPPIV in the renal brush-border microdomains of Y-SHR, A-SHR, and age-matched WKY rats. Equal quantities (20 µg protein) of MMV and IMV prepared from Y (*A, C, E,* and *G*)- or A (*B, D, F,* and *H*)-SHR and WKY rat kidneys by density fractionation of postmitochondrial microsomes were analyzed by immunoblotting. Blots were probed with antibodies to villin (*A* and *B*), megalin (*C* and *D*), NHE3 (*E* and *F*), and DPPIV (*G* and *H*). Values are means ± SE; $n = 5$/group; *$P < 0.01$ vs. MMV-WKY, #$P < 0.01$ and ##$P < 0.05$ vs. IMV-WKY.

performed in the native PT in contrast to cell culture models (21) or ex vivo preparations (25). Although in vitro models are very valuable tools to isolate and dissect single effects, the applicability of them for the elucidation of integrative physiological and pathological processes may be limited. Furthermore, inhibition of NHE3 activity in the A-SHR may depend on factors, which may not be present or functional in ex vivo preparations. In line with our findings, Panico et al. (35) very recently demonstrated that PT fluid reabsorption is reduced in the A-SHR by ~60% compared with age-matched WKY. The authors proposed that diminished fluid reabsorption in the A-SHR was related to increased reactive oxygen species, since direct microperfusion of reducing agents restored PT transport function in these animals (35).

Numerous studies have aimed to investigate the molecular basis for sodium retention in the SHR kidney. With regard to NHE3 modulation, most of these reports have not found significant differences of NHE3 transcripts or protein abundance between SHR and normotensive strains (20, 31, 35, 46). In agreement with this, we have not noticed any significant variation of the levels of NHE3 expression between SHR and same-age WKY rats. Interestingly, NHE3-mRNA and protein expression were significantly higher in both A-SHR and A-WKY rats relative to their young counterparts. This increment is probably due to the developmental changes of NHE isoforms in postnatal PT (3). Although NHE3 function and expression increased concurrently with age in the WKY, such direct correlation could not be observed in the SHR (Table 2). It implies that changes of NHE3 activity during the age interval of 5 to 14 wk in the hypertensive rat strain are mainly caused by posttranslational mechanisms.
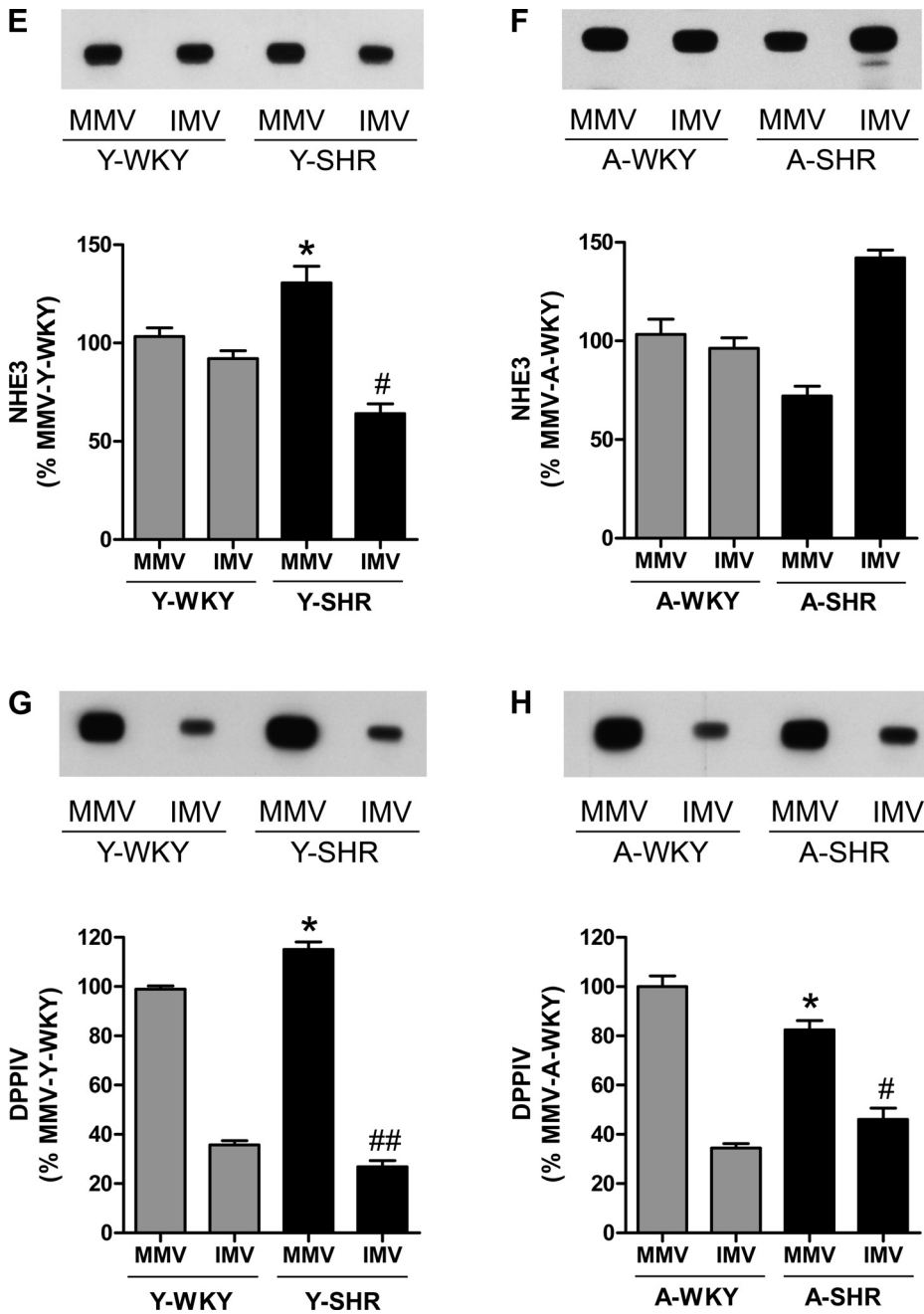
E

F

Fig. 5—*Continued*

G

H

Phosphorylation of the serine-552 residue in the COOH-terminal region of NHE3 seems to be necessary for PKA to exert inhibition of the exchanger (23). One of the major new findings of our study is that changes in NHE3 activity occur concurrently with changes of NHE3 phosphorylation status in the SHR model. In prehypertensive Y-SHR, the relative ratio of P-NHE3/total in renal cortical microsomes were significantly lower compared with WKY (~70%) and similar in magnitude to NHE3 transport stimulation (~80%). When considering this quotient in terms of age dependence, the P-NHE3/total ratio increased with age in SHR (~70%), correlating well with the reduction of NHE3 activity (~60%). These results suggest that increased NHE3 function in the Y-SHR PT is attributable to abnormalities in signaling pathways that either

prevent activation of kinases or overactivate phosphatases. There is evidence that the ability of dopamine-1 receptor agonists to inhibit NHE3 in renal PT and induce natriuresis is impaired in the SHR (29). In these animals, the dopamine-1 receptor is uncoupled from its effector adenylyl cyclase and thus fails to activate PKA. Changes in the phosphorylation status of renal proteins involved in sodium transport are not unprecedented. Similar to NHE3, the phosphorylation of the Na^+/K^+-ATPase α-1 subunit at serine-18 is decreased in the Y-SHR PT (17). This altered pattern of phosphorylation increases the recruitment of the α-1 subunit of the Na^+/K^+-ATPase to the basolateral membrane and consequently enhances PT sodium reabsorption (26). It has been postulated that increased apical sodium entry via NHE3 induces a coordinate

rise in the activity of the Na^+/K^+-ATPase contributing to sodium retention and blood pressure rising in the Y-SHR (17). The finding that elevation of intracellular sodium concentration leads to Na^+/K^+-ATPase dephosphorylation strengthens this hypothesis (19).

Inhibition of NHE3 by cAMP requires the presence of either NHE regulatory factor-1 (NHERF1) or NHERF2 to allow the catalytic subunit of PKA II to phosphorylate NHE3 (24, 48). It has been previously shown that NHERF2 expression is increased at both protein (35) and mRNA levels (21) after development of hypertension in the SHR PT. The higher expression of the PDZ scaffold protein NHERF2 may be related to the higher levels of phosphorylated NHE3 and reduced activity of the transporter in the A-SHR renal cortex.

Phosphorylation of the 552 residue of NHE3 has been implicated in NHE3 subcellular trafficking (22, 23). Accordingly, we found that in prehypertensive Y-SHR, MMV NHE3 expression is higher than in the IMV cleft. Conversely, in hypertensive A-SHR, NHE3 is mainly confined to the IMV microdomain. Our data support those of other laboratories (31, 45, 46) that have demonstrated that acute and chronic hypertension provoke redistribution of NHE3 from the body to the base of MMV.

We previously discovered that a significant pool of NHE3 physically associates with DPPIV in renal PT (10) and that inhibition of DPPIV downregulates NHE3 activity (11, 12). A variety of conditions that affect salt balance and change NHE3 subcellular localization alters DPPIV distribution as well (28, 31, 44–46), including a coordinate redistribution of DPPIV and NHE3 out of the MMV-enriched membranes during the development of hypertension in the SHR (31). Thus it is conceivable that assembly of NHE3 with DPPIV is lower when the NHE3-mediated Na^+/H^+ exchange is reduced. These observations also suggest that the peptidase may also play a role in volume homeostasis and blood pressure control. In line with this observation, our laboratory has recently demonstrated that exendin-4, an agonist of the glucagon-like peptide-1 (GLP-1) receptor, inhibits NHE3 activity in PT cells (7). GLP-1 is a DPPIV substrate, and it has been shown by us and others to be involved in sodium homeostasis (7, 14, 15, 18, 34, 47). Of note, both GLP-1 and exendin-4 have antihypertensive actions (18, 47). Whether inhibition of DPPIV may attenuate the rising of blood pressure and whether this is due to increased GLP-1 half-life remains to be determined.

NHE3 and DPPIV do not directly bind to each other, indicating that additional accessory proteins are required for the association to occur (13). It is conceivable that one of these accessory proteins mediates the dynamic subcellular trafficking of the NHE3-DPPIV complex in response to physiological and pathophysiological stimuli. In fact, Leong et al. (28) have demonstrated that the cytoskeleton proteins myosin-IIA (nonmuscle) and myosin VI retract out of the MMV along with NHE3 and DPPIV in response to the ACE inhibitor captopril. Further studies are needed to evaluate whether these molecular motor proteins are capable of physically associating with NHE3 and DPPIV.

We conclude that NHE3 activity decreases with age in the SHR, while increasing with age in the WKY. The fall in activity in SHR is associated with an increase in direct phosphorylation of the transporter and subcellular distribution out of the MMV along with its regulator DPPIV. The elucidation of the signaling pathways that control phosphorylation of sodium transport proteins and of binding partners that mediate their subcellular trafficking may unravel important mechanisms implicated in the pathophysiology of essential hypertension.

DISCLOSURES

No conflicts of interest, financial or otherwise, are declared by the author(s).

REFERENCES

1. **Aronson PS.** Energy-dependence of phlorizin binding to isolated renal microvillus membranes. Evidence concerning the mechanism of coupling between the electrochemical Na^+ gradient the sugar transport. *J Membr Biol* 42: 81–98, 1978.
2. **Aronson PS, Giebisch G.** Mechanisms of chloride transport in the proximal tubule. *Am J Physiol Renal Physiol* 273: F179–F192, 1997.
3. **Becker AM, Zhang J, Goyal S, Dwarakanath V, Aronson PS, Moe OW, Baum M.** Ontogeny of NHE8 in the rat proximal tubule. *Am J Physiol Renal Physiol* 293: F255–F261, 2007.
4. **Biemesderfer D, DeGray B, Aronson PS.** Active (9.6 s) and inactive (21 s) oligomers of NHE3 in microdomains of the renal brush border. *J Biol Chem* 276: 10161–10167, 2001.
5. **Biemesderfer D, Pizzonia J, Abu-Alfa A, Exner M, Reilly R, Igarashi P, Aronson PS.** NHE3: a Na^+/H^+ exchanger isoform of renal brush border. *Am J Physiol Renal Fluid Electrolyte Physiol* 265: F736–F742, 1993.
6. **Biemesderfer D, Rutherford PA, Nagy T, Pizzonia JH, Abu-Alfa AK, Aronson PS.** Monoclonal antibodies for high-resolution localization of NHE3 in adult and neonatal rat kidney. *Am J Physiol Renal Physiol* 273: F289–F299, 1997.
7. **Carraro-Lacroix LR, Malnic G, Girardi AC.** Regulation of Na^+/H^+ exchanger NHE3 by glucagon-like peptide 1 receptor agonist exendin-4 in renal proximal tubule cells. *Am J Physiol Renal Physiol* 297: F1647–F1655, 2009.
8. **Fernandez R, Lopes MJ, de Lira RF, Dantas WF, Cragoe Junior EJ, Malnic G.** Mechanism of acidification along cortical distal tubule of the rat. *Am J Physiol Renal Fluid Electrolyte Physiol* 266: F218–F226, 1994.
9. **Fisher KA, Lee SH, Walker J, Dileto-Fang C, Ginsberg L, Stapleton SR.** Regulation of proximal tubule sodium/hydrogen antiporter with chronic volume contraction. *Am J Physiol Renal Physiol* 280: F922–F926, 2001.
10. **Girardi AC, Degray BC, Nagy T, Biemesderfer D, Aronson PS.** Association of Na^+-H^+ exchanger isoform NHE3 and dipeptidyl peptidase IV in the renal proximal tubule. *J Biol Chem* 276: 46671–46677, 2001.
11. **Girardi AC, Fukuda LE, Rossoni LV, Malnic G, Reboucas NA.** Dipeptidyl peptidase IV inhibition downregulates Na^+-H^+ exchanger NHE3 in rat renal proximal tubule. *Am J Physiol Renal Physiol* 294: F414–F422, 2008.
12. **Girardi AC, Knauf F, Demuth HU, Aronson PS.** Role of dipeptidyl peptidase IV in regulating activity of Na^+/H^+ exchanger isoform NHE3 in proximal tubule cells. *Am J Physiol Cell Physiol* 287: C1238–C1245, 2004.
13. **Girardi AC, Thomson RB, Aronson PS.** Identification of domain of Na/H exchanger NHE3 mediating association with dipeptidyl peptidase IV (DPPIV) (Abstract). *FASEB J* 19: 140A, 2005.
14. **Gutzwiller JP, Hruz P, Huber AR, Hamel C, Zehnder C, Drewe J, Gutmann H, Stanga Z, Vogel D, Beglinger C.** Glucagon-like peptide-1 is involved in sodium and water homeostasis in humans. *Digestion* 73: 142–150, 2006.
15. **Gutzwiller JP, Tschopp S, Bock A, Zehnder CE, Huber AR, Kreyenbuehl M, Gutmann H, Drewe J, Henzen C, Goeke B, Beglinger C.** Glucagon-like peptide 1 induces natriuresis in healthy subjects and in

insulin-resistant obese men. *J Clin Endocrinol Metab* 89: 3055–3061, 2004.

16. **Hayashi M, Yoshida T, Monkawa T, Yamaji Y, Sato S, Saruta T.** Na$^+$/H$^+$-exchanger 3 activity and its gene in the spontaneously hypertensive rat kidney. *J Hypertens* 15: 43–48, 1997.

17. **Hinojos CA, Doris PA.** Altered subcellular distribution of Na$^+$,K$^+$-ATPase in proximal tubules in young spontaneously hypertensive rats. *Hypertension* 44: 95–100, 2004.

18. **Hirata K, Kume S, Araki S, Sakaguchi M, Chin-Kanasaki M, Isshiki K, Sugimoto T, Nishiyama A, Koya D, Haneda M, Kashiwagi A, Uzu T.** Exendin-4 has an anti-hypertensive effect in salt-sensitive mice model. *Biochem Biophys Res Commun* 380: 44–49, 2009.

19. **Ibarra FR, Cheng SX, Agren M, Svensson LB, Aizman O, Aperia A.** Intracellular sodium modulates the state of protein kinase C phosphorylation of rat proximal tubule Na$^+$,K$^+$-ATPase. *Acta Physiol Scand* 175: 165–171, 2002.

20. **Kim SW, Wang W, Kwon TH, Knepper MA, Frokiaer J, Nielsen S.** Increased expression of ENaC subunits and increased apical targeting of AQP2 in the kidneys of spontaneously hypertensive rats. *Am J Physiol Renal Physiol* 289: F957–F968, 2005.

21. **Kobayashi K, Monkawa T, Hayashi M, Saruta T.** Expression of the Na$^+$/H$^+$ exchanger regulatory protein family in genetically hypertensive rats. *J Hypertens* 22: 1723–1730, 2004.

22. **Kocinsky HS, Dynia DW, Wang T, Aronson PS.** NHE3 phosphorylation at serines 552 and 605 does not directly affect NHE3 activity. *Am J Physiol Renal Physiol* 293: F212–F218, 2007.

23. **Kocinsky HS, Girardi AC, Biemesderfer D, Nguyen T, Mentone S, Orlowski J, Aronson PS.** Use of phospho-specific antibodies to determine the phosphorylation of endogenous Na$^+$/H$^+$ exchanger NHE3 at PKA consensus sites. *Am J Physiol Renal Physiol* 289: F249–F258, 2005.

24. **Lamprecht G, Weinman EJ, Yun CH.** The role of NHERF and E3KARP in the cAMP-mediated inhibition of NHE3. *J Biol Chem* 273: 29972–29978, 1998.

25. **LaPointe MS, Sodhi C, Sahai A, Batlle D.** Na$^+$/H$^+$ exchange activity and NHE-3 expression in renal tubules from the spontaneously hypertensive rat. *Kidney Int* 62: 157–165, 2002.

26. **Lecuona E, Dada LA, Sun H, Butti ML, Zhou G, Chew TL, Sznajder JI.** Na,K-ATPase α1-subunit dephosphorylation by protein phosphatase 2A is necessary for its recruitment to the plasma membrane. *FASEB J* 20: 2618–2620, 2006.

27. **Ledoussal C, Lorenz JN, Nieman ML, Soleimani M, Schultheis PJ, Shull GE.** Renal salt wasting in mice lacking NHE3 Na$^+$/H$^+$ exchanger but not in mice lacking NHE2. *Am J Physiol Renal Physiol* 281: F718–F727, 2001.

28. **Leong PK, Devillez A, Sandberg MB, Yang LE, Yip DK, Klein JB, McDonough AA.** Effects of ACE inhibition on proximal tubule sodium transport. *Am J Physiol Renal Physiol* 290: F854–F863, 2006.

29. **Li XX, Xu J, Zheng S, Albrecht FE, Robillard JE, Eisner GM, Jose PA.** D$_1$ dopamine receptor regulation of NHE3 during development in spontaneously hypertensive rats. *Am J Physiol Regul Integr Comp Physiol* 280: R1650–R1656, 2001.

30. **Lorenz JN, Schultheis PJ, Traynor T, Shull GE, Schnermann J.** Micropuncture analysis of single-nephron function in NHE3-deficient mice. *Am J Physiol Renal Physiol* 277: F447–F453, 1999.

31. **Magyar CE, Zhang Y, Holstein-Rathlou NH, McDonough AA.** Proximal tubule Na transporter responses are the same during acute and chronic hypertension. *Am J Physiol Renal Physiol* 279: F358–F369, 2000.

32. **Meneton P, Jeunemaitre X, de Wardener HE, MacGregor GA.** Links between dietary salt intake, renal salt handling, blood pressure, and cardiovascular diseases. *Physiol Rev* 85: 679–715, 2005.

33. **Moe OW, Tejedor A, Levi M, Seldin DW, Preisig PA, Alpern RJ.** Dietary NaCl modulates Na$^+$-H$^+$ antiporter activity in renal cortical apical membrane vesicles. *Am J Physiol Renal Fluid Electrolyte Physiol* 260: F130–F137, 1991.

34. **Moreno C, Mistry M, Roman RJ.** Renal effects of glucagon-like peptide in rats. *Eur J Pharmacol* 434: 163–167, 2002.

35. **Panico C, Luo Z, Damiano S, Artigiano F, Gill P, Welch WJ.** Renal proximal tubular reabsorption is reduced in adult spontaneously hypertensive rats: roles of superoxide and Na$^+$/H$^+$ exchanger 3. *Hypertension* 54: 1291–1297, 2009.

36. **Puissant C, Houdebine LM.** An improvement of the single-step method of RNA isolation by acid guanidinium thiocyanate-phenol-chloroform extraction. *Biotechniques* 8: 148–149, 1990.

37. **Schultheis PJ, Clarke LL, Meneton P, Miller ML, Soleimani M, Gawenis LR, Riddle TM, Duffy JJ, Doetschman T, Wang T, Giebisch G, Aronson PS, Lorenz JN, Shull GE.** Renal and intestinal absorptive defects in mice lacking the NHE3 Na$^+$/H$^+$ exchanger. *Nat Genet* 19: 282–285, 1998.

38. **Schwark JR, Jansen HW, Lang HJ, Krick W, Burckhardt G, Hropot M.** S3226, a novel inhibitor of Na$^+$/H$^+$ exchanger subtype 3 in various cell types. *Pflügers Arch* 436: 797–800, 1998.

39. **Thomas D, Harris PJ, Morgan TO.** Age-related changes in angiotensin II-stimulated proximal tubule fluid reabsorption in the spontaneously hypertensive rat. *J Hypertens Suppl* 6: S449–S451, 1988.

40. **Vallon V, Schwark JR, Richter K, Hropot M.** Role of Na$^+$/H$^+$ exchanger NHE3 in nephron function: micropuncture studies with S3226, an inhibitor of NHE3. *Am J Physiol Renal Physiol* 278: F375–F379, 2000.

41. **Wang T, Hropot M, Aronson PS, Giebisch G.** Role of NHE isoforms in mediating bicarbonate reabsorption along the nephron. *Am J Physiol Renal Physiol* 281: F1117–F1122, 2001.

42. **Wang T, Yang CL, Abbiati T, Schultheis PJ, Shull GE, Giebisch G, Aronson PS.** Mechanism of proximal tubule bicarbonate absorption in NHE3 null mice. *Am J Physiol Renal Physiol* 277: F298–F302, 1999.

43. **Warnock DG, Yee VJ.** Chloride uptake by brush border membrane vesicles isolated from rabbit renal cortex. Coupling to proton gradients and K+ diffusion potentials. *J Clin Invest* 67: 103–115, 1981.

44. **Yang LE, Leong PK, McDonough AA.** Reducing blood pressure in SHR with enalapril provokes redistribution of NHE3, NaPi2, and NCC and decreases NaPi2 and ACE abundance. *Am J Physiol Renal Physiol* 293: F1197–F1208, 2007.

45. **Yang LE, Sandberg MB, Can AD, Pihakaski-Maunsbach K, McDonough AA.** Effects of dietary salt on renal Na$^+$ transporter subcellular distribution, abundance, and phosphorylation status. *Am J Physiol Renal Physiol* 295: F1003–F1016, 2008.

46. **Yip KP, Tse CM, McDonough AA, Marsh DJ.** Redistribution of Na$^+$/H$^+$ exchanger isoform NHE3 in proximal tubules induced by acute and chronic hypertension. *Am J Physiol Renal Physiol* 275: F565–F575, 1998.

47. **Yu M, Moreno C, Hoagland KM, Dahly A, Ditter K, Mistry M, Roman RJ.** Antihypertensive effect of glucagon-like peptide 1 in Dahl salt-sensitive rats. *J Hypertens* 21: 1125–1135, 2003.

48. **Yun CH, Oh S, Zizak M, Steplock D, Tsao S, Tse CM, Weinman EJ, Donowitz M.** cAMP-mediated inhibition of the epithelial brush-border Na$^+$/H$^+$ exchanger, NHE3, requires an associated regulatory protein. *Proc Natl Acad Sci USA* 94: 3010–3015, 1997.